Information processing using a single Izhikevich neuron

Tomoyuki Kubota[1], Kohei Nakajima[2] and Hirokazu Takahashi[3]

[1]Department of Advanced Interdisciplinary Studies, Graduate School of Engineering, The University of Tokyo
[2]Graduate School of Information Science and Technology, The University of Tokyo,
JST, PRESTO, 4-1-8 Honcho, Kawaguchi, Saitama 332-0012, Japan
[3] Research Center for Advanced Science and Technology, The University of Tokyo
4-6-1 Komaba, Meguro-ku, Tokyo, 153-8904, Japan
kubota@brain.imi.i.u-tokyo.ac.jp

Abstract

How does a single spiking neuron process information? This question is a long lasting one, which has been constantly posed and pursued by many researchers from different perspectives. In this paper, we tackle this issue from the perspective of reservoir computing using a single Izhikevich neuron as a model system. To prepare reservoir nodes from the response of a single Izhikevich neuron, we used of a technique called time multiplexing, which exploits a time-scale difference between input-output series and the transient dynamics of the single neuron. Based on this scheme, we evaluated the information processing capability of a single Izhikevich neuron using a standard benchmark task. Furthermore, we measured its memory capacity and showed its characteristic memory profile in various parameter settings. Finally, the relationships between the dynamical properties of the Izhikevich neuron and its memory capacity are discussed in detail.

Introduction

Neurons compose neural circuits and understanding their information processing capability is an interesting research subject. The computational capability of a single neuron has been evaluated quantitatively in various ways.

Neurons are thought to process input information with action potentials. Blaise et al. and Hong et al. investigated the input-output relationship of spiking neurons by means of white noise analysis and clarified the features that spiking neurons extracted with action potentials (Blaise et al., 2003 and Hong et al., 2007). Although a spiking neuron is often described as an integrate-and-fire model, it is not possible to sufficiently express with an integrator or a threshold (Blaise et al., 2003). Schmitt tried to reproduce the action potential of spiking neurons with McCulloch-Pitts neurons and evaluated the computational capacity of spiking neurons with the number of thresholds necessary for reproduction (Schmitt, 1998).

Zador et al. evaluated the ability of the action potential of the leaky integrate-and-fire model to classify inputs using the VC dimension (Zador et al., 1996). Maass showed the condition under which a simplified integrate-and-fire model classifies inputs robustly (Maass, 1997). Šíma et al. showed that the VC dimension of spiking neurons is higher than that of perceptron (Šíma et al., 2005).

In this paper, we focus on the computational capability of a spiking neuron from a novel viewpoint. We introduce a framework of reservoir computing (RC) (Jaeger et al., 2004; Maass et al., 2007; Verstraeten et al., 2007), which allows one to exploit dynamical systems as computational resources, to examine this problem. In RC, each computing element called the node, has a response, and each node mutually couples to form a network referred to as the reservoir. The computational capacity is composed of memory capacity and nonlinearity and a reservoir carries out computation using present and past stored inputs. Given time series inputs to the reservoir, after each node response is calculated, the output is determined by linear regression. One can compose a generator of an arbitrary time series signal with the reservoir, determining the regression coefficient properly.

We composed a reservoir with a single spiking neuron using a method referred to as "time multiplexing" (e.g., Appeltant et al., 2011; Larger et al., 2012). This method allows one to supply a huge number of computational nodes from a single time series, making use of the timescale difference between input-output computation and the dynamics of a single spiking neuron. Similar procedures have been utilized for the reservoirs, whose number of computational nodes are physically constrained and difficult to be increased spatially (e.g., Fujii et al., 2017; Nakajima et al., 2018a; Nakajima et al., 2018b). In this paper, we focus on a single Izhikevich neuron as a model system and evaluate the computational capability of the reservoir with various parameter settings of the Izhikevich neuron. For the analysis, we used a standard benchmark task and measured the memory capacity of the system.

Methods

Izhikevich Neuron

The cerebral neocortex is composed of excitatory and inhibitory neurons. Based on electrophysiological characteristics, excitatory neurons are classified into three types: regular spiking (RS), intrinsically bursting (IB) and chattering (CH). Inhibitory neurons are also classified into three types: late spiking (LS), low-threshold spiking (LTS) and

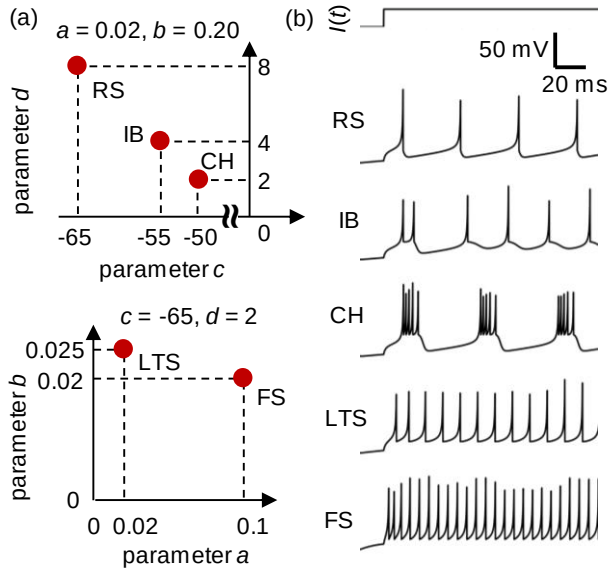

Figure 1: Izhikevich neuron. (a) Parameters to determine the type of neuron. (b) Responses of typical neurons in the neocortex. The RS neuron continuously fires with spike frequency adaptation. The IB neuron bursts right after input, and then continuously fires. The CH neuron bursts repeatedly. The LTS and FS neurons frequently fire with and without spike frequency adaptation, respectively. The input current was constant $I = 10$.
RS: regular spiking, IB: intrinsically bursting, CH: chattering, LTS: low-threshold spiking, FS: fast spiking

fast spiking (FS) (Connors et al., 1990; Gray et al., 1996; Gibson et al., 1999). Izhikevich expressed the response of RS, IB, CH, LTS and FS neurons by combining differential equations and a conditional branch (Izhikevich, 2003). The dynamics of Izhikevich neurons are described as:

$$\frac{dv}{dt} = 0.04v^2 + 5v + 140 - u + I, \tag{1}$$

$$\frac{du}{dt} = a(bv - u), \tag{2}$$

$$\text{if } v \geq 30 \text{ mV}, \begin{cases} v \leftarrow c \\ u \leftarrow u + d' \end{cases} \tag{3}$$

where v is the membrane potential and u is the membrane recovery variable. a, b, c and d are parameters determining the response of the neuron. Figure 1 shows the parameters (a, b, c, d) to determine the type of neuron and the response characteristics of the neuron.

The Izhikevich neuron is so rich in expressing responses that adjusting parameters enables the model to reproduce a variety of responses (Izhikevich, 2004). The large number of parameters of a neuron model makes it difficult to locate a region where the model has high computational capacity, but it is possible to use only four parameters. For these two reasons, we adopted the Izhikevich neuron to investigate the computational capacity of a single spiking neuron.

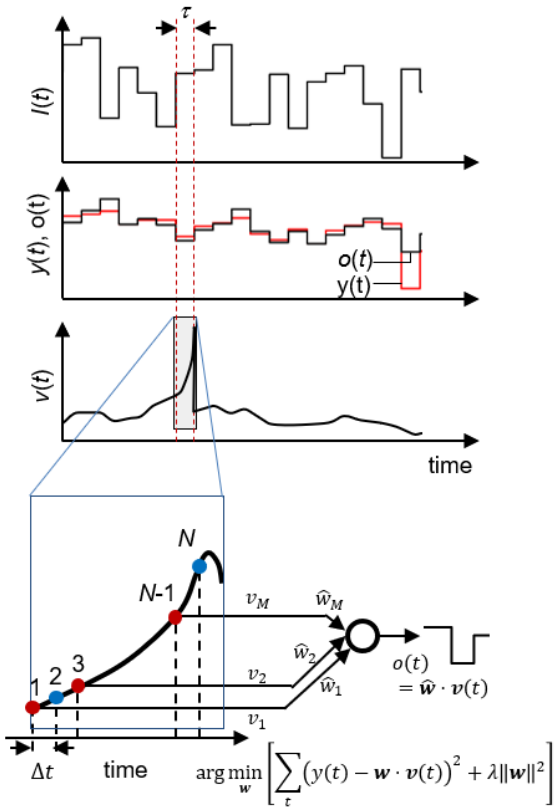

Figure 2: Composing a reservoir of a single Izhikevich neuron with time multiplexing

Composing a Reservoir Using a Single Neuron

In order to use a single Izhikevich neuron as a reservoir, time multiplexing was adopted (Appeltant et al., 2011). As shown in Figure 2, the input current $I(t)$ is fixed during each time window τ and we divided the i-th time window $(i = 0, 1, \cdots)$ into 2^m time steps and defined $M\ (= 2^m)$ virtual nodes as membrane voltages at the time steps $t = i\tau + j(\tau/M)$ $(j = 0, 1, \cdots, M-1)$. To calculate Eqs. (1)-(3) with time width Δt fixed regardless of M, we also divided the τ into $N\ (= 2^n)$ time steps more finely than $M\ (= 2^m)$ $(n \geq m)$ and set the time window width as $\tau = N\Delta t$. Eq. (4) shows the vector representation of the virtual nodes in the i-th time window $(i = 0, 1, \cdots)$.

$$\boldsymbol{v}_i = \begin{bmatrix} v(i\tau) \\ v\left(i\tau + \frac{M}{N}\Delta t\right) \\ \vdots \\ v\left(i\tau + \frac{(N-1)M}{N}\Delta t\right) \end{bmatrix} \tag{4}$$

The membrane potential obtained by Eqs. (1)-(3) has an initial transient and using this for training may increase the evaluation error. Thus, we set a washout phase, a learning phase, and an evaluation phase, to $i = 0, \cdots, 999$, $i = 1000, \cdots, 1999$, and $i = 2000, \cdots, 2999$, respectively, and discarded 1000 steps in the washout phase. For learning, we employed Ridge

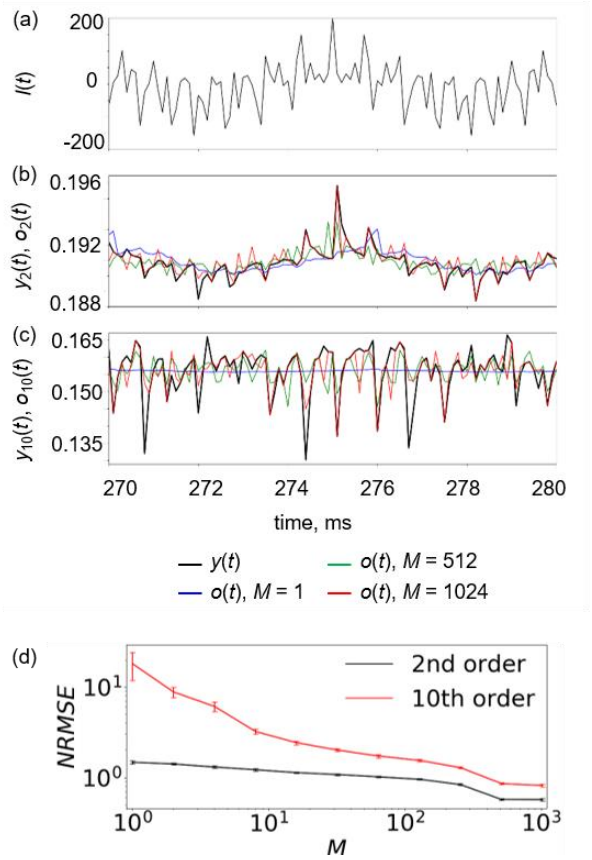

Figure 3: Emulation of nonlinear autoregressive-moving average models. (a) Input time series data. (b) The second order nonlinear system. (c) The tenth order nonlinear system. In Figures 3(b) and (c), the bold and thin lines represent the target output and the output of the reservoir, respectively. (d) Relationship between M and the averaged $NRMSE$ of the second and tenth order nonlinear system. The error bars stand for the standard deviations. NRMSE: normalized root mean square error

regression, by which weights $\widehat{\boldsymbol{w}}$ were calculated in Eq. (5). The output o_i at the i-th time window is shown in Eq. (6).

$$\widehat{\boldsymbol{w}} = \arg\min_{\boldsymbol{w}} \left\{ \sum_{i=1000}^{1999} \frac{(y_i - \boldsymbol{w}\cdot\boldsymbol{v}_i)^2}{1000} + \alpha\|\boldsymbol{w}\|_2^2 \right\}, \tag{5}$$

$$o_i = \widehat{\boldsymbol{w}}\cdot\boldsymbol{v}_i, \tag{6}$$

where y_i represents the target output at time window i, $||\cdot||_2$ is the Euclidean norm and α is a hyper parameter that adjusts the degree of normalization and employs a minimum value of mean square error (MSE) of the evaluation data:

$$\sum_{i=2000}^{2999} \frac{(y_i - \widehat{\boldsymbol{w}}\cdot\boldsymbol{v}_i)^2}{1000}. \tag{7}$$

Evaluation Methods

NARMA models To confirm the computational capability of the reservoir, we attempted to emulate two nonlinear autoregressive moving average (NARMA) models (Atiya et al., 2000; Jaeger et al., 2004; Verstraeten et al., 2007). We used the functions shown in Eqs. (8) and (9) and evaluated the normalized root mean square error (NRMSE) between the target output and the reservoir output.

$$y(t) = 0.4y(t-1) + 0.4y(t-1)y(t-2) + 0.6in(t-1)^3 + 0.1 \tag{8}$$

$$y(t) = 0.3y(t-1) + 0.05y(t-1)\left[\sum_{i=1}^{10} y(t-i)\right] + 1.5in(t-10)in(t-1) + 0.1 \tag{9}$$

Note that Eq. (8) is a second order nonlinear system and Eq. (9) is a tenth order nonlinear system. The input $in(t)$ of Eqs. (8) and (9) is given as follows:

$$in(t) = 0.2\sin(2\pi f_1 \Delta t * t) * \sin(2\pi f_2 \Delta t * t) * \sin(2\pi f_3 \Delta t * t), \tag{10}$$

where f_1, f_2, f_3 and Δt are set to 2.11,. 3.73, 4.33 and 0.1, respectively. The input $in(t)$ to the NARMA models is transformed into the input $I(t)$ to the Izhikevich neuron as follows:

$$I(t) = w_{in} * in(t), \tag{11}$$

where w_{in} is set to 1000. The NRMSE is defined as

$$NRMSE = \sqrt{\sum_{i=2000}^{2999} \frac{(y_i - \widehat{\boldsymbol{w}}\cdot\boldsymbol{v}_i)^2}{1000 sd^2(\widehat{\boldsymbol{w}}\cdot\boldsymbol{v}_i)}}, \tag{12}$$

where $sd(\widehat{\boldsymbol{w}}\cdot\boldsymbol{v}_i)$ is the standard deviation of $\widehat{\boldsymbol{w}}\cdot\boldsymbol{v}_i$ $(i = 2000, \cdots 2999)$. We ran each task for 50 trials and averaged $NRMSE$.

Memory capacity The memory capacity (Jaeger, 2001) is a measure to evaluate the short-term memory of a reservoir, representing the quantity of past input information in a reservoir. A uniform random number on the interval $[0, \sigma]$ is set as input $I(t)$, and $I(t - i\tau)$ $(i = 1,2,\cdots,10)$ the input delayed by i time windows is set as the target output y_i.

$\widehat{\boldsymbol{w}}_i$ is a weight vector such that for each target output, the coefficient of determination $d[\boldsymbol{w}_i](o_i, y_i)$ is maximized (Eq. 13). Let the maximum value be memory function MF_i (Eq. 14) and let the sum over the maximum value be MC (Eq. 15).

$$d[\boldsymbol{w}_i](y_i, o_i) = \frac{cov^2(y_i, o_i)}{sd^2(y_i)\cdot sd^2(o_i)}, \tag{13}$$

$$MF_i = \max_{\boldsymbol{w}_i} d[\boldsymbol{w}_i](y_i, o_i), \tag{14}$$

$$MC = \sum_{i=1}^{10} MF_i, \tag{15}$$

where $cov(\cdot)$ denotes covariance and $sd(\cdot)$ stands for standard deviation.

Lyapunov exponent The Lyapunov exponent reveals the stability or chaoticity of dynamical systems. We investigated the response property of the Izhikevich neuron by calculating the Lyapunov exponent of Eqs. (1)-(3) as the input is a uniform random number. The Izhikevich neuron is a hybrid system, in which a continuous-time system and a discrete-time system coexist and usually draws a continuous trajectory, which

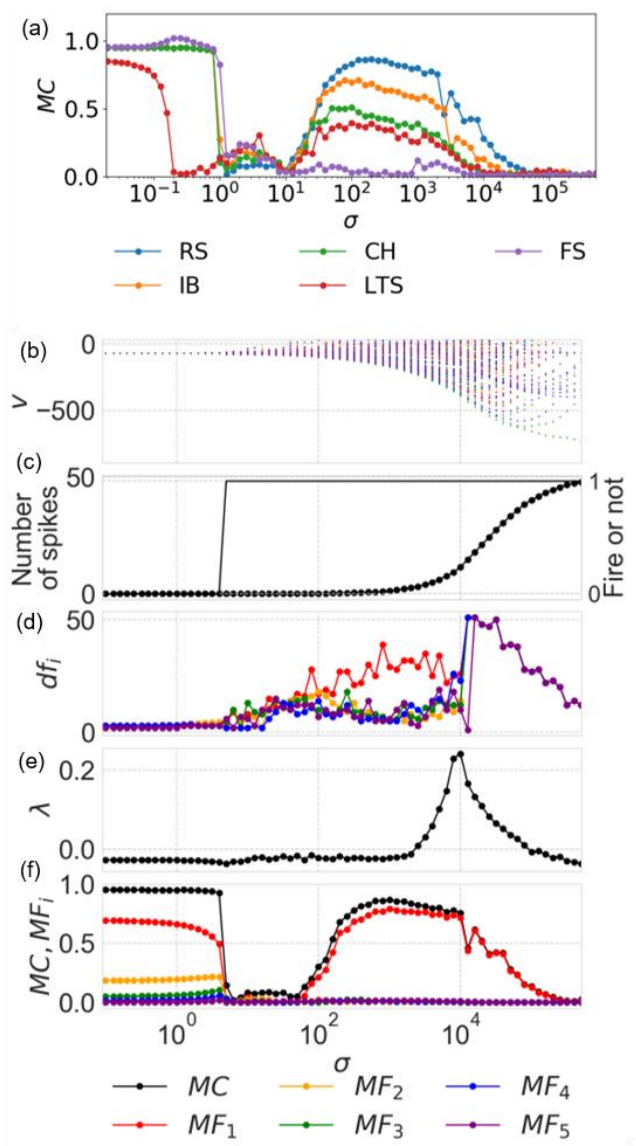

Figure 4: (a) Relationship between the input intensity σ and MC in typical neurons (RS, IB, CH, LTS, and FS). (b) Bifurcation diagram of membrane potential v. The relationship between σ and v in the five typical virtual nodes are plotted in different colors. (c) The average number of spikes in a time window and whether the neuron fires or not at the σ. When the neuron fires or not, the value is 1 or 0, respectively. (d) Relationship between σ and the effective degrees of freedom df_i $(i = 1,2,3,4,5)$, whose colors correspond to the colors of MF_i $(i = 1,2,3,4,5)$ in Figure 4(f). (e) Relationship between σ and the Lyapunov exponent λ. (f) Relationship between σ and MC, and σ and MF_i $(i = 1,2,3,4,5)$.
RS: regular spiking, IB: intrinsically bursting, CH: chattering, LTS: low-threshold spiking, FS: fast spiking, MC: memory capacity, MF: memory function

becomes discrete at a spiking time. To calculate the Lyapunov exponent for such a system, a method using a saltation matrix was proposed (Bizzarri et al., 2013). In this method, the state transition matrix $\boldsymbol{\Phi}_{k+1}(t, t_k)$ between the k-th and $(k+1)$-th spiking is expressed as

$$\frac{d}{dt}\boldsymbol{\Phi}_{k+1}(t, t_k) = \boldsymbol{J}(v, u, t)\boldsymbol{\Phi}_{k+1}(t, t_k), \tag{16}$$

$$\boldsymbol{\Phi}_{k+1}(t_k, t_k) = \boldsymbol{E}, \tag{17}$$

where $\boldsymbol{J}$ is the Jacobian matrix of Eqs. (1) and (2) and $\boldsymbol{E}$ is the identity matrix. The saltation matrix $\boldsymbol{S}_k$ is given by

$$\boldsymbol{S}_k = \begin{bmatrix} \frac{\dot{v}^+}{\dot{v}^-} & 0 \\ \frac{(\dot{u}^+ - \dot{u}^-)}{\dot{v}^-} & 1 \end{bmatrix}, \tag{18}$$

where (v^-, u^-) and (v^+, u^+) are (v, u) at a time step $t = t_k$ before and after spiking, respectively.

When the neuron fires i times on the interval $[T^k, T^{k+1}]$, the ordinary differential equation of the state transition matrix $\boldsymbol{\Phi}_{i+1}(t, t_i)$ is given as follows:

$$\begin{aligned}\boldsymbol{\Phi}^k(T^{k+1}, T^k) = \boldsymbol{\Phi}_{i+1}(T^{k+1}, t_i)\boldsymbol{S}_i\boldsymbol{\Phi}_i(t_i, t_{i-1}) \\ \cdots \boldsymbol{S}_2\boldsymbol{\Phi}_2(t_2, t_1)\boldsymbol{S}_1\boldsymbol{\Phi}_1(t_1, T^k).\end{aligned} \tag{19}$$

The Lyapunov spectrum λ_j $(j = 1, 2)$ is calculated with eigenvalues l_k^j $(j = 1, 2)$ of $\boldsymbol{\Phi}_{i+1}(t, t_i)$ as follows:

$$\lambda_j = \frac{1}{N}\sum_{k=0}^{N-1}\frac{1}{T^{k+1} - T^k}\log\left(\left|l_j^k\right|\right), \tag{20}$$

where we follow the setting of Nobukawa et al. (2017) and set $T^{k+1} - T^k$ to 1000 ms in the case that $T^{k+1} - T^k$ lasts for 1000 ms before 20 spikes occur; otherwise $T^{k+1} - T^k$ is set to the time required for 20 spikes.

Results

NARMA Models

To confirm that a single neuron can be used as a reservoir, we attempted to emulate two NARMA models: the second order and the tenth order nonlinear systems. These models are complicated dynamical systems determined by the past state variables and past and present inputs. Let the number of virtual nodes M be a power of two, $1, 2, 4, \cdots, 1024$ and we investigated how the number of virtual nodes affects the ability to emulate NARMA models. Note that time window τ is set to 102.4 ms and the number of partitions N is set to 1024. The parameters of the Izhikevich neuron are $(a, b, c, d) = (0.02, 0.2, -65, 8)$ and the RS neuron is employed as a reservoir.

As shown in Figure 3(b), the reservoir with $M = 512, 1024$ accurately emulates the target output ($NRMSE = 0.567$ with $M = 512$ and $NRMSE = 0.555$ with $M = 1024$). The reservoir with $M = 1$, however, emulates the low frequency band of the target output and caused a large error ($NRMSE = 1.43$). As the output of the reservoir with $M = 512, 1024$ includes a higher frequency band, NRMSE emphasizes the emulation performance, dividing the root mean square error by the standard deviation.

As shown in Figure 3(c), the emulation of the tenth order nonlinear system also reflects the same trend. The reservoir with $M = 1$ emulates only the low frequency band of the target output ($NRMSE = 14.4$). On the other hand, as $M = 512, 1024$, the reservoir output emulates the high frequency

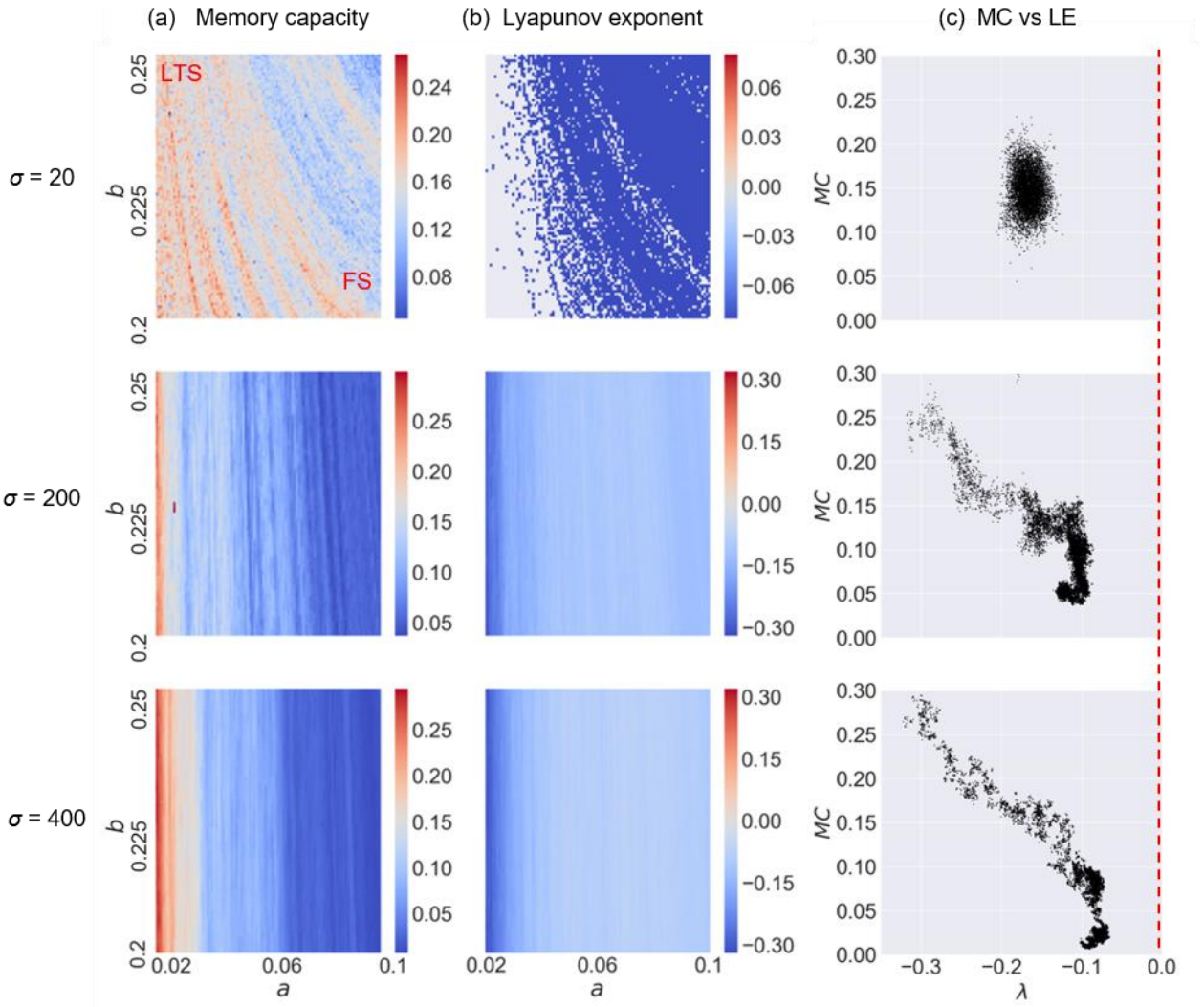

Figure 5: Computational capacity and response characteristics of a single Izhikevich neuron in the inhibitory region. (a) Memory capacity. (b) Maximal Lyapunov exponent. (c) Relationship between memory capacity and Lyapunov exponent. MC: memory capacity, LE: Lyapunov exponent, LTS: low-threshold spiking, FS: fast spiking

band ($NRMSE = 0.841$ with $M = 512$ and $NRMSE = 0.84$ with $M = 1024$).

In Figure 3(d), monotonical decreases in NRMSEs of the second and tenth nonlinear systems show that a large number of virtual nodes certainly decrease the emulation errors, which indicates that this method to supply nodes is effective in improving the performance of emulation.

Memory Capacity

The computational capability of a single Izhikevich neuron was evaluated quantitatively with memory capacity. The five types of neurons (Figure 1) were utilized as reservoirs and their computational capacities were compared. The input was a uniform random number on the interval $[0, \sigma]$.

Figure 4(a) shows the relationship between the σ and MC of each neuron. Note that $\tau = 1$ ms, $N = 50$, $M = 50$. All neurons share the characteristic profile that MC is large at small σ, but when σ becomes larger than a specific value, MC sharply decreases. This sudden decrease in the MC of RS, IB, CH, LTS and FS neurons occurred at $\sigma = 5.0$, 5.0, 5.0, 1.0 and 6.3, respectively. As σ further increases, MC increases until MC achieves local maximum value and decreases after the local maxima.

Legenstein and Maass (2007) argued that it is not possible to discuss information processing capability only by means of the edge of chaos and that it is possible to use a method to examine the linear separation property of dynamics by means of a rank. In order to investigate the cause of this profile in MC, we calculated the effective degrees of freedom as a rank. When Ridge regression is adopted, the effective degrees of freedom are described as:

$$df_k(\alpha_k) = \sum_{i=1}^{M+1} \frac{\lambda_i}{\lambda_i + \alpha_k}, \tag{21}$$

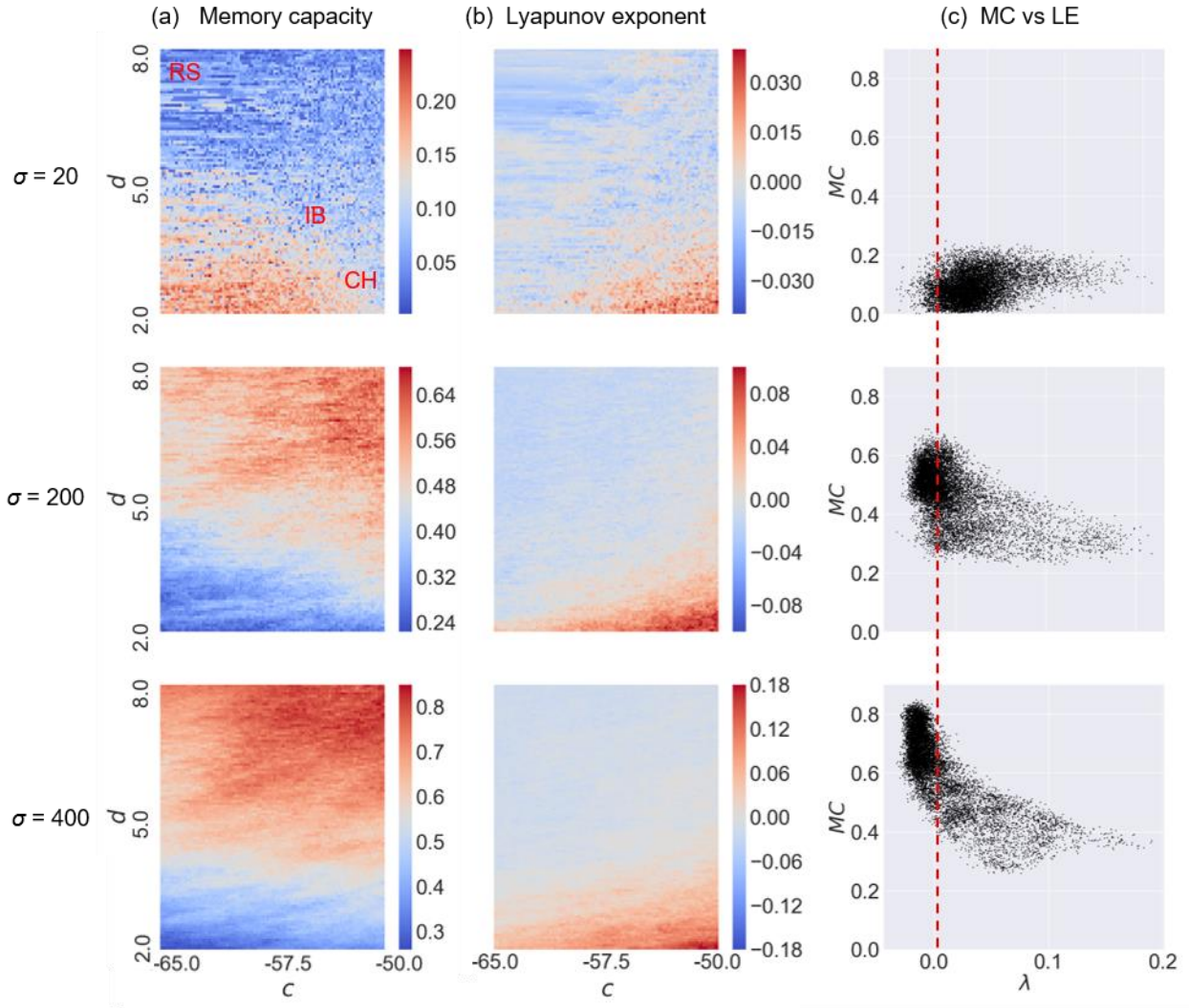

Figure 6: Computational capacity and response characteristics of a single Izhikevich neuron in the excitatory region. (a) Memory capacity. (b) Maximal Lyapunov exponent. (c) Relationship between memory capacity and Lyapunov exponent.
MC: memory capacity, LE: Lyapunov exponent, RS: regular spiking, IB: intrinsically bursting, CH: chattering

where λ_i $(i = 1, \cdots, M+1)$ are the eigenvalues of the matrix $\boldsymbol{v} \cdot \boldsymbol{v}^T$ with $\boldsymbol{v}$ the vector representation of virtual nodes and α_k $(k = 1, \cdots, 10)$ are the hyper parameters of Ridge regression to emulate the input delayed by k time windows. Since the range of df_k is zero to $M+1$, we calculate α_k when df_k is a natural number $(1, 2, \cdots, M+1)$, obtain the MSE for each α_k and choose the α_k that realizes the smallest MSE among them.

As shown in Figure 4(b), (c) and (f), RS does not spike at $\sigma \leq 5.0$, where MC is large. Note that the firing thresholds σ of RS, IB, CH, LTS and FS neurons are 5.0, 5.0, 5.0, 1.0 and 6.3, respectively. As shown in Figure 4(d) and (e), since the effective degrees of freedom for $i = 1, \cdots, 5$ are less than 7 at $\sigma \leq 5.0$, the virtual nodes contain a small number of regular and independent responses, which achieve a high MC.

At the smallest σ where an action potential occurs ($\sigma = 5.0$), MC decreases nonlinearly, which is affected by the nonlinearity of the neuron dynamics. Since Eq. (3) is calculated when the neuron fires, the cause is the conditional branch.

After an action potential occurs ($\sigma > 5.0$), as the effective degree of freedom for $i = 1$ gradually increases and the response becomes regular, the linear separation property of the input is improved and MC increases until $\sigma = 1.11 \times 10^3$. Because the Lyapunov exponent λ changes from negative to positive at $\sigma = 1.17 \times 10^3$ and the response becomes chaotic (noise induced chaos (Crutchfield et al., 1980; Tél et al., 2008)), MC is maximized in the vicinity of $\lambda = 0$ (edge of chaos). After λ becomes positive, as the input intensity increases, the response becomes unstable and λ continues to increase but begins to descend after $\sigma = 1.0 \times 10^4$, where the neuron

receives such large input that the conditional branch occurs at successive time steps and membrane potential may be fixed to c. Note that the successive spikes maximize the effective degrees of freedom for $i = 1, \cdots, 5$ but the many independent responses are chaotic and have almost no computational capacity. For this reason, λ begins to decrease and becomes negative again (noise induced order (Matsumoto et al., 1983)). Since the membrane potential is fixed to c, MC decreases to zero.

Accordingly, the memory capacity profile is unique to the hybrid system, whose conditional branch causes the sudden decrease in MC and the decrease in MC after the local maxima.

The relationships between σ and MC differ in each type of neuron, which indicates that the computational capacity of each neuron depends on the parameters to determine the dynamical response of the Izhikevich neuron. Although we calculated the memory capacities of the five typical neurons, actual neurons in the neocortex have rich diversity. Therefore, the parameters (a, b, c, d) of the Izhikevich neuron were exhaustively changed and memory capacities with these parameters were calculated.

Izhikevich set parameter regions of excitatory and inhibitory neurons, accounting for heterogeneity (Izhikevich, 2003). The area of excitatory neurons is $a = 0.02, b = 0.2, -65 \leq c \leq -50, 2 \leq d \leq 8$, including RS, IB and CH neurons. On the other hand, the area of inhibitory neurons is $0.02 \leq a \leq 0.1, 0.2 \leq b \leq 0.25, c = -65, d = 2$, and LTS and FS neurons are included in this area. Figures 5 and 6 show the memory capacity MC and the Lyapunov exponent λ at $\sigma = 20, 200, 400$ in the inhibitory area and in the excitatory area, respectively. Note that $\tau = 0.9$ ms, $N = 9$, and $M = 9$.

As shown in Figure 5 in the inhibitory region, at $\sigma = 20$, when action potentials rarely occur, the memory capacity and the Lyapunov exponent complicatedly change, depending on both parameters a and b, and the response is always regular because the λ is negative. By contrast, at $\sigma = 200, 400$, that is, when an action potential is frequently generated, neither MC nor λ has dependency on parameter b. This is because the recovery variable u becomes much larger ($|u| \gg |bv|$). Besides, the smaller a is, the larger MC is, and the smaller λ is; therefore, MC conflicts with λ. Figure 6 shows that the dependency of excitatory neurons on the parameters c, d is small at $\sigma = 20$. However, at $\sigma = 200$ and 400, MC tends to increase as c and d increase. As c increases and d decreases, λ becomes larger at $\sigma = 20, 200$ and 400. At $\sigma = 20$, 200 and 400, MC becomes maximum at positive λ, at around $\lambda = 0$ and at negative λ, respectively. This implies that when an excitatory neuron rarely fires ($\sigma = 20$), the chaotic responses have computational capacity and that as the firing rate increases, the response becomes regular, which has more computational capacity.

These results indicate that the regular response characteristics of a single neuron reservoir have large computational capacity in both excitatory and inhibitory neurons.

Discussion

The results of this study imply the memory capacity property of a single spiking neuron. It should be noted that evaluation by reservoir does not express purely computing capacity of a single neuron because time multiplexing increases the number of nodes. However, this computational capacity reflects the dynamics of a single spiking neuron. As shown in Figure 4(f), when the neuron fires, MC is composed almost entirely of MF_1, implying that firing neurons may hold only the input delayed by one time window. Moreover, from Figure 5(a), in a case where a large input is provided to the inhibitory neuron, MC is large when a is small; that is, decay of the recovery variable is slow. As can be seen from Figure 6(a), in a case where a large input is provided to an excitatory neuron, MC is large when both c and d are large; that is, the resting membrane potential is large and the initial offset of decay in the recovery variable is large.

In this paper, we used the framework of reservoir computing to evaluate the computational capacity of a single spiking neuron. For the Izhikevich neuron model, however, the nonlinearity of the conditional branch has a large influence on the profile of the memory capacity of the input intensity σ. Although the Izhikevich neuron is a model that reproduces physiologically measured responses, this discontinuous component may have effects that do not occur in actual responses. It is expected that a phenomenon similar to the sharp decrease in MC appears in other spiking neuron models. Future research should compare the memory capacity profiles of various spiking neuron models.

We used a single spiking neuron as a reservoir with time multiplexing. Although this method of reservoir composition may enable one to use a single Izhikevich neuron as a reservoir, a large memory capacity is required to emulate context-dependent tasks. In this study, we found that the memory capacity of the reservoir was less than one. The maximum value of memory capacity is equal to the effective degree of freedom (Jaeger, 2001), which is large when a large number of responses in nodes are not combined linearly and we can exploit more computational capacity in the region where nonlinear effects in Eqs. (1)-(3) appear. Candidates to improve memory capacity are as follows: (1) Tuning τ the width of the time window can nonlinearly change the virtual nodes; (2) As proposed in a reservoir with a laser system (Appeltant et al., 2011), changing the input weight at each time step in a time window may increase the number of independent responses, which also increases MF_i and MC.

Conclusions

In this study, we aimed to compose a reservoir with a single spiking neuron using time multiplexing. For various parameter settings of the Izhikevich neuron, the computational capacity of the reservoir was quantitatively evaluated with two measures: the ability to emulate the NARMA models and the memory capacity. The results were as follows:

- The reservoir emulates the NARMA models, which shows that time multiplexing may be used to construct a reservoir with a single Izhikevich neuron.
- One of the causes of the unique memory capacity profile is the nonlinearity of the conditional branch.
- The memory capacity of a single Izhikevich neuron reservoir has a complicated dependency on input intensity σ.

- The memory capacity of a single Izhikevich neuron reservoir also has a complicated dependency on the four parameters (a, b, c, d). Regular response characteristics have large computational capacity in both excitatory and inhibitory neurons.

Acknowledge

We would like to acknowledge Hitachi UTokyo Laboratory, Hitachi, Ltd. for fruitful discussions. K.N. was supported by JST PRESTO Grant Number JPMJPR15E7, Japan, and KAKENHI No. 15K16076 and No. 26880010.

References

Appeltant, L., Soriano, M. C., Van der Sande, G., Danckaert, J., Massar, S., Dambre, J., ... & Fischer, I. (2011). Information processing using a single dynamical node as complex system. Nature communications, 2, 468.

Arcas, B. A. Y., Fairhall, A. L., & Bialek, W. (2003). Computation in a single neuron: Hodgkin and Huxley revisited. Neural Computation, 15(8), 1715-1749.

Atiya, A. F., & Parlos, A. G. (2000). New results on recurrent network training: unifying the algorithms and accelerating convergence. IEEE transactions on neural networks, 11(3), 697-709.

Bizzarri, F., Brambilla, A., & Gajani, G. S. (2013). Lyapunov exponents computation for hybrid neurons. Journal of computational neuroscience, 35(2), 201-212.

Connors, B. W., & Gutnick, M. J. (1990). Intrinsic firing patterns of diverse neocortical neurons. Trends in neurosciences, 13(3), 99-104.

Crutchfield, J. P., & Huberman, B. A. (1980). Fluctuations and the onset of chaos. Physics Letters A, 77(6), 407-410.

Fujii, K., & Nakajima, K. (2017). Harnessing Disordered-Ensemble Quantum Dynamics for Machine Learning. Physical Review Applied, 8(2), 024030.

Gibson, J. R., Beierlein, M., & Connors, B. W. (1999). Two networks of electrically coupled inhibitory neurons in neocortex. Nature, 402(6757), 75.

Gray, C. M., & McCormick, D. A. (1996). Chattering cells: superficial pyramidal neurons contributing to the generation of synchronous oscillations in the visual cortex. Science, 274(5284), 109-113.

Hong, S., Agüera y Arcas, B., & Fairhall, A. L. (2007). Single neuron computation: from dynamical system to feature detector. Neural computation, 19(12), 3133-3172.

Izhikevich, E. M. (2003). Simple model of spiking neurons. IEEE Transactions on neural networks, 14(6), 1569-1572.

Izhikevich, E. M. (2004). Which model to use for cortical spiking neurons?. IEEE transactions on neural networks, 15(5), 1063-1070.

Jaeger, H. (2001). Short term memory in echo state networks (Vol. 5). GMD-Forschungszentrum Informationstechnik.

Jaeger, H., & Haas, H. (2004). Harnessing nonlinearity: Predicting chaotic systems and saving energy in wireless communication. science, 304(5667), 78-80.

Larger, L., Soriano, M. C., Brunner, D., Appeltant, L., Gutiérrez, J. M., Pesquera, L., ... & Fischer, I. (2012). Photonic information processing beyond Turing: an optoelectronic implementation of reservoir computing. Optics express, 20(3), 3241-3249.

Legenstein, R., & Maass, W. (2007). Edge of chaos and prediction of computational performance for neural circuit models. Neural Networks, 20(3), 323-334.

Maass, W., & Schmitt, M. (1997, July). On the complexity of learning for a spiking neuron. In Proceedings of the tenth annual conference on Computational learning theory (pp. 54-61). ACM.

Maass, W., Natschläger, T., & Markram, H. (2002). Real-time computing without stable states: A new framework for neural computation based on perturbations. Neural computation, 14(11), 2531-2560.

Matsumoto, K., & Tsuda, I. (1983). Noise-induced order. Journal of Statistical Physics, 31(1), 87-106.

Nakajima, K., Fujii, K., Negoro, M., Mitarai, K., & Kitagawa, M. (2018a). Boosting computational power through spatial multiplexing in quantum reservoir computing. arXiv preprint arXiv:1803.04574.

Nakajima, K., Hauser, H., Li, T., & Pfeifer, R. (2018b). Exploiting the Dynamics of Soft Materials for Machine Learning. Soft Robotics, http://doi.org/10.1089/soro.2017.0075.

Nobukawa, S., Nishimura, H., & Yamanishi, T. (2017). Chaotic resonance in typical routes to chaos in the Izhikevich neuron model. Scientific reports, 7(1), 1331.

Schmitt, M. (1998). On computing Boolean functions by a spiking neuron. Annals of Mathematics and Artificial Intelligence, 24(1-4), 181-191.

Šíma, J., & Sgall, J. (2005). On the nonlearnability of a single spiking neuron. Neural Computation, 17(12), 2635-2647.

Tél, T., Lai, Y. C., & Gruiz, M. (2008). Noise-induced chaos: a consequence of long deterministic transients. International Journal of Bifurcation and Chaos, 18(02), 509-520.

Verstraeten, D., Schrauwen, B., d'Haene, M., & Stroobandt, D. (2007). An experimental unification of reservoir computing methods. Neural networks, 20(3), 391-403.

Zador, A. M., & Pearlmutter, B. A. (1996, January). VC dimension of an integrate-and-fire neuron model. In Proceedings of the ninth annual conference on Computational learning theory (pp. 10-18). ACM.